

**NORTH PACIFIC GYRE OSCILLATION
SYNCHRONIZES CLIMATE FLUCTUATIONS IN THE
EASTERN AND WESTERN BOUNDARY SYSTEMS**

A Thesis
Presented to
The Academic Faculty

by

Lina I. Ceballos

In Partial Fulfillment
of the Requirements for the Degree
Master of Sciences in the
School of Earth and Atmospheric Sciences

Georgia Institute of Technology
December 2008

**NORTH PACIFIC GYRE OSCILLATION
SYNCHRONIZES CLIMATE FLUCTUATIONS IN THE
EASTERN AND WESTERN BOUNDARY SYSTEMS**

Approved by:

Dr. Emanuele Di Lorenzo, Advisor
School of Earth and Atmospheric Sciences
Georgia Institute of Technology

Dr. Annalisa Bracco
School of Earth and Atmospheric Sciences
Georgia Institute of Technology

Dr. Peter J. Webster
School of Earth and Atmospheric Sciences
Georgia Institute of Technology

Date Approved: November 14, 2008

ACKNOWLEDGEMENTS

I would like to thank the people who have contributed to this work; specially Drs. Emanuele Di Lorenzo and Carlos D. Hoyos for their support and guidance. I also would like to thank my committee members Drs. Annalisa Braco and Peter Webster for their time and comments.

TABLE OF CONTENTS

ACKNOWLEDGEMENTS	iii
LIST OF FIGURES	v
SUMMARY	vi
I INTRODUCTION	1
II PACIFIC DECADEAL VARIABILITY (PDV)	4
2.1 Mechanisms of Pacific Decadal Variability	5
2.2 The Pacific Decadal Oscillation (PDO) and North Pacific Gyre Oscillation (NPGO)	7
III DATA	9
IV KOE DECADEAL VARIABILITY	10
V DYNAMICS AND PROCESSES	13
VI SUMMARY AND CONCLUSIONS	18

LIST OF FIGURES

1	(a) EOF-1 and (b) EOF-2 of monthly sea level pressure anomalies during 1950-2004 over the North Pacific and its associated principal components PC-1 (c) and PC-2 (d). The EOFs explain 32.5 and 18.7% of the total SLP variance. The thick lines represent a 12 month running mean.	1
2	(a) Correlation map between the NPGO index and the OFES SSHa in the North Pacific (shaded contours). The red box delimits the region where the NPGO index was obtained. The contour lines represent the mean sea level. (b) Time series of the NPGO index (red line), and SSHa gradient in the black box on the left. This gradient represents the strength of the central/eastern branches of the subpolar and subtropical gyres.	8
3	Time series of the second mode of variability in the KOE (blue curve), and SSHa gradient in the KOE region which corresponds to the strength of the Kuroshio Extension jet.	10
4	(a) NPGO (red) and KOE mode-2 (blue). The NPGO time axis is shifted 2.5 years forward in time to match the time of the maximum correlation coefficient between the two time series as shown on (b) . .	11
5	Spatial correlation pattern between (a) KOE mode-2 and OFES SSHa at 0 year lag and (b) at lag -3 yr (KOE leading). (c) Spatial correlation between NPGO and SSH anomalies at lag 0. (d) Time-longitude section at 35.25N (black line on the left panel) of the lagged correlation maps between KOE mode-2 and SSHa.	11
6	Time-longitude plots of SSHa averaged between 32.38-38.09N for (a) satellite data, (b) OFES hindcast, and (c) wind stress curl forced Rossby wave model. The yellow, red, and black boxes correspond to the KOE region where SSHa was averaged to obtain the time series in (d).	14
7	Time-longitude plots of SSHa averaged between 32.38-38.09N from (a) the Aleutian Low mode, and (b) the NPO related wind stress curl anomalies forced Rossby wave model.	15
8	(a) Aleutian Low related KOE SSHa time series (red curve) and (b) NPO related KOE SSHa time series (blue curve). The black curve is the KOE SSHa time series from OFES.	16

9	Wind stress curl correlation maps with the NPO as defined by Linkin and Nigam (2008) (a) and the NPO index defined by Chhak et al. (2008) (b). (c-d) Time series of the NPO index defined by these authors respectively and, (e-f) reconstructions of the NPGO index (black curve) using an AR-1 and the NPO indices as predictors.	17
---	---	----

SUMMARY

Recent studies have identified the North Pacific Gyre Oscillation (NPGO) as a decadal mode of climate variability that is linked to previously unexplained fluctuations of salinity, nutrient, and chlorophyll in the Northeast Pacific. The NPGO reflects changes in strength of the central and eastern branches of the subtropical gyre and is driven by the atmosphere through the North Pacific Oscillation (NPO) -the second dominant mode of sea level pressure variability. We show that Rossby waves dynamics excited by the NPO propagate the NPGO signature from the central North Pacific into the Kuroshio-Oyashio Extension (KOE), and trigger changes in strength of the KOE with a lag of 3 years. This suggests that the NPGO index can be used to track changes in the entire northern branch of the North Pacific sub-tropical gyre. These results also provide a physical mechanism to explain coherent decadal climate variations and ecosystem changes between the North Pacific eastern and western boundaries.

CHAPTER I

INTRODUCTION

Decadal timescale climate variability in the North Pacific has received considerable attention in the recent years because of its impact on tropical and extratropical climate (e.g. Deser et al. 1999; Graham 1994); weather over North America (e.g. Latif and Barnett 1994; Barlow et al. 2001); and regional marine ecosystems (e.g. Mantua et al. 1997; Francis et al. 1998; Fiedler 2002). Analyses of sea level pressure (SLP) data suggest that, on decadal timescales, there are two dominant modes of atmospheric variability in the North Pacific. The first one (Figure 1a) is associated with changes in the Aleutian Low (e.g. Trenberth and Hurrell 1994). The second one (Figure 1b) is termed the North Pacific Oscillation (NPO; Walker and Bliss 1932).

In the central North Pacific, a strengthened Aleutian Low is associated with a decrease of sea surface temperature (SST) as a result of cold air advection from the north, increase of ocean-atmosphere turbulent heat fluxes, and by equatorward advection of temperature from Ekman currents. In the eastern North Pacific, a deepened Aleutian Low intensifies poleward winds leading to warm SST anomalies along the west coast of North America, the Gulf of Alaska, and across the eastern subtropics and tropics (Schneider and Cornuelle 2005). Changes in the Aleutian Low also affect the western Pacific since anomalous wind stress curl in the central Pacific forces the circulation to change and baroclinic Rossby waves to propagate from the central North Pacific to the western boundary, arriving several years after the Aleutian Low changes, resulting in a lagged SST response in the Kuroshio-Oyashio Extension (KOE) region (Miller et al. 2004). The pattern of SST anomalies associated to the Aleutian Low variability is consistent with the spatial pattern of the Pacific

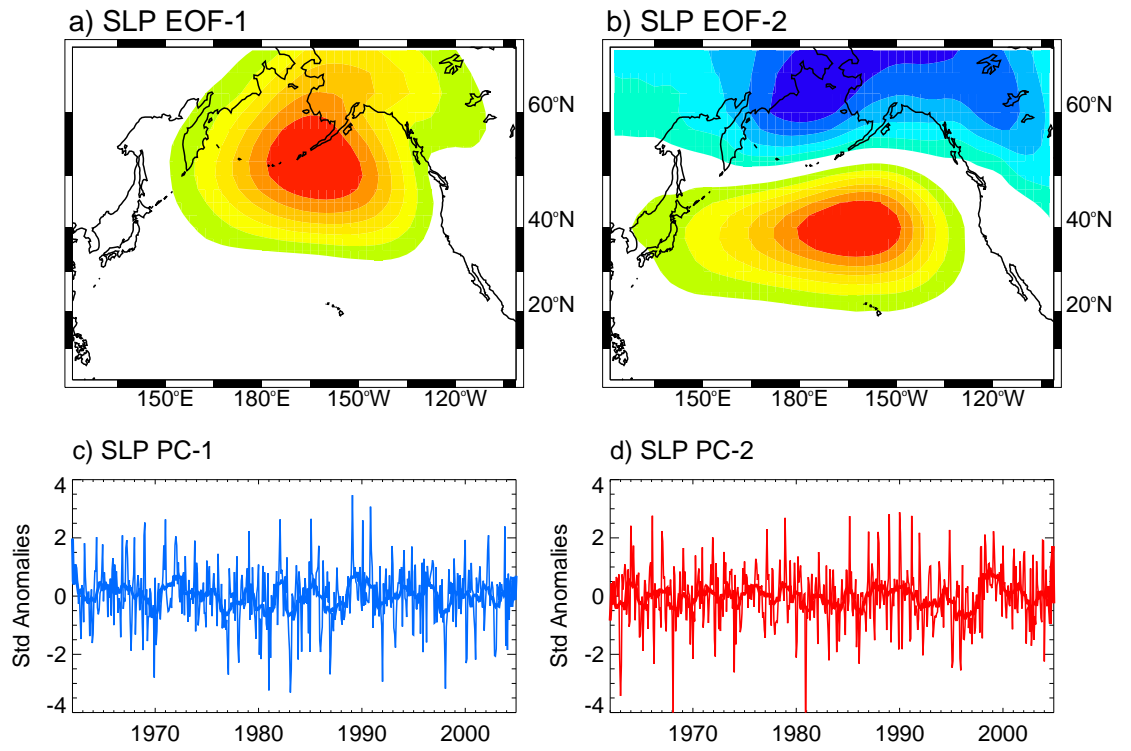


Figure 1: (a) EOF-1 and (b) EOF-2 of monthly sea level pressure anomalies during 1950-2004 over the North Pacific and its associated principal components PC-1 (c) and PC-2 (d). The EOFs explain 32.5 and 18.7% of the total SLP variance. The thick lines represent a 12 month running mean.

Decadal Oscillation (PDO; Mantua et al. 1997), defined as the leading empirical orthogonal function (EOF) of SST anomalies in the Pacific (north of 20°N). This pattern similarity has led to studies linking PDO to changes in the atmospheric SLP following the earlier study by Davis (1976). Using an AR-1 processes, Schneider and Cornuelle (2005) and Chhak et al. (2008) found that SLP anomalies in the Aleutian low had high skill in reconstructing the observed PDO amplitude.

In contrast to the Aleutian Low mode, the NPO spatial pattern consists of a dipole structure in which SLP variations in the central Pacific near Hawaii oppose those over Alaska (Figure 1b). Walker and Bliss (1932) found significant correlation between the NPO and precipitation and surface air temperature anomalies over North America and Asia. Rogers (1981) linked the NPO with the advance and retreat of sea ice edge in the Bering Sea. Chiang and Vimont (2004) linked the NPO with the Pacific meridional mode and with forcing of ENSO via the SST footprint mechanism (Vimont et al. 2001, 2003). Recently, Chhak et al. (2008) found that the NPO has an oceanic expression termed the North Pacific Gyre Oscillation (NPGO, Di Lorenzo et al. 2008) that is evident from an analysis of sea surface height anomalies (SSHa) in the Northeast Pacific and is correlated with previously unexplained fluctuation of salinity, nutrient, and chlorophyll observations in the Northeast Pacific.

In this study, we explore the relationship between decadal variations in the eastern and western boundary current systems of the North Pacific Ocean. Specifically, we show how NPGO variability in the central and eastern North Pacific is connected to decadal variations in the KOE with a phase lag of approximately 3 years. We explore this connection using both a statistical and a dynamical approach. The statistical approach involves time-lagged spatial correlation maps that show how the NPGO pattern propagates westward in the KOE, where it tracks decadal variations in the strength of the KOE. The dynamical approach explores the east-west relationship using a simple linear Rossby wave model. The role of Rossby wave dynamics in

explaining climate variability of the KOE has been pointed out in several studies (e.g. Qiu 2003; Schneider et al. 2002; Seager et al. 2001). Using a reduced gravity model, Qiu (2003) tracked the baroclinic oceanic response back to surface winds and showed that variability on the Kuroshio Extension is remotely forced by wind stress anomalies in the eastern/central North Pacific. We follow Qiu’s methodology to explore if the NPO - the forcing of the NPGO - modulates SSHa variability on the western boundary. To do this we decompose the wind stress into two components, one associated with the Aleutian Low mode and one related with the NPO. This allows us to assess the relative contribution of the two dominant atmospheric forcing modes on SSHa variability in the KOE. We also use SSH data from satellite and from a high resolution eddy-resolving model hindcast of the OFES (OGCM for the Earth Simulator; Masumoto et al. 2004; Sasaki et al. 2008). The OFES model captures realistically the decadal variations in the KOE (Taguchi et al. 2007) as well as the NPGO pattern (Figure 2a).

This manuscript is organized as follows. Chapter 2 contains a brief review on the Pacific decadal variability theories and mechanisms. Chapter 3 describes the observational and modeling datasets used in this study. Chapter 4 examines the statistical relationship between the NPGO and low-frequency variability in the KOE using the OFES model hindcast. Chapter 5 shows the results from the Rossby wave model and a comparison with SSHa from satellite and OFES. Discussions and conclusions are given in Chapter 6.

CHAPTER II

PACIFIC DECADEAL VARIABILITY (PDV)

Decadal variations in climate can occur as gradual drifts, smooth oscillations, or step-like shifts. During 1976-77, a step-like shift in the climate system occurred in the Pacific Ocean (e.g. Miller et al. 1994; Nitta and Yamada 1989; Trenberth 1990). Large-scale atmospheric and oceanic changes were observed in the North Pacific Ocean which include a deepening in the Aleutian Low, a drop in SST in the central Pacific, and a rise in SST in the eastern Pacific. A few years later a cooling was observed in the western Pacific in the Kuroshio-Oyashio Extension (KOE) region. This climate shift led to extensive studies of the PDV focusing on both the atmospheric and oceanic patterns of this variability with SST and SLP being the typically used variables because they have the longest observational records.

As mentioned before, statistical analyses of observed SST and SLP have allowed the establishment of dominant atmospheric and oceanic patterns of the North Pacific on decadal time scales. In the atmosphere, the dominant pattern is associated with changes in the Aleutian Low (Trenberth and Hurrell 1994), whereas in the ocean the SST pattern is the response to surface forcing by the atmospheric wind stress field associated with changes in the Aleutian Low (Miller et al. 1994). Analyses of SST data have revealed that there are two dominant modes of variability: the first one is characterized by a cold (warm) region in the central North Pacific and a warm (cold) pattern along the eastern coast of North America for a strengthened (weakened) Aleutian Low. This mode is known as the ENSO mode since it is remotely forced by teleconnected ENSO signals (Alexander 1992; Alexander et al. 2002; Deser and Blackmon 1995). The second mode, known as the North Pacific mode, has

its center of action in the western North Pacific around 40°N (Kuroshio-Oyashio Extension, KOE, region) and is associated with intrinsic processes of the midlatitude North Pacific (Deser and Blackmon 1995; Nakamura et al. 1997). Even though the dominant patterns of PDV have been established, its causes and mechanisms are not well understood, and several hypotheses have been proposed to explain the observed decadal variability.

2.1 Mechanisms of Pacific Decadal Variability

On decadal time scales SST variability in the North Pacific can be generated through three different mechanisms. The simplest explanation suggests that stochastic variations in the atmospheric forcing drive long-term oceanic changes. Under this scenario, a white-noise surface heat flux forcing may reproduce SST spectral peaks at decadal time scales (Hasselmann 1976; Frankignoul and Hasselmann 1977). The other mechanisms involve atmospheric teleconnections from the tropics and midlatitude ocean-atmosphere interactions.

The relationship between tropical Pacific SST anomalies during ENSO events and North Pacific SST anomalies has been suggested by Alexander (1992); Alexander et al. (2002); Deser and Blackmon (1995); and Weare et al. (1976), among others. The linkage between the two regions is thought to occur via the atmosphere. Anomalous convection over the equatorial Pacific associated with ENSO induces a remote atmospheric circulation response over the North Pacific that changes the surface heat, momentum, freshwater fluxes, and later the SST via mixed layer dynamics. Thus, the atmosphere acts as a bridge spanning from the equatorial Pacific to the North Pacific (Alexander et al., 2002). These processes have been invoked to explain some aspects of the 1976-77 climate shift in the North Pacific (Graham 1994; Miller et al. 1994; Trenberth 1990).

Deser and Blackmon (1995) and Alexander et al. (2002) showed that the canonical SST pattern over the eastern/central North Pacific is highly correlated with variability in the tropical SST. In particular, Alexander et al. (2002) showed that the time evolution of the eastern/central North Pacific pattern is highly correlated with tropical Pacific SST indices used to represent ENSO variability. In contrast, Deser and Blackmon (1995) and Nakamura et al. (1997) found that the second dominant mode of SST variability in the North Pacific, concentrated along the subarctic front in the western North Pacific, is uncorrelated with tropical SST variability and concluded that other mechanisms such as midlatitude ocean-atmosphere interactions are responsible for the observed decadal variability in the KOE region.

The midlatitude ocean-atmosphere interactions hypothesis was proposed by Latif and Barnett (1994, 1996) to explain variability in a coupled general circulation model (CGCM) with periods around 20 years. This hypothesis has been studied by Schneider and Miller (2001), Pierce et al. (2001), Kwon and Deser (2007), and Qiu et al. (2007), among others using various long-term CGCM runs. All the results have pointed out the importance of the KOE region in controlling the SST variability on the western North Pacific.

According to Latif and Barnett (1994; 1996), a spin-up of the subtropical gyre will bring anomalous warm waters from the tropics into the region inducing positive SSTAs in the KOE. These anomalies may then feed back to the atmosphere spinning down the gyre after a lag of many years, reversing the sign of the SSTAs there. According to this hypothesis, after the 1976-77 shift cooling of the central Pacific a warming of the KOE was expected, but observations suggest that indeed there was a cooling in the KOE region instead of a warming. The cooling in the KOE region was clearly associated with the gyre-scale response to wind stress curl forcing, but the origin of these patterns is unclear (Miller and Schneider 2000). An alternative interpretation of this mechanism was offered by Miller and Schneider (2000) who suggested that since

both the subtropical and subarctic gyre are spun-up by an anomalous strong Aleutian Low, increasing downwelling and upwelling on each gyre respectively, one of the two gyres has to become dominant to achieve the observed KOE SSTa. In relation with the 1976-77 shift, the subarctic gyre may be more important than the subtropical one since a cooling of the KOE region was observed (Miller et al. 1998). Results by Pierce et al. (2001) and Qiu et al. (2007) suggest that indeed an ocean-atmosphere feedback is necessary to reproduce the observed SST decadal variability in the KOE region.

Additional theories have been proposed for decadal variability in the North Pacific which include oceanic teleconnections via Kelvin wave-like disturbances coming from the Tropics (Meyers et al. 1996), variations along tropical-subtropical subduction paths that may alter the state of the tropical ocean-atmosphere system (Gu and Philander 1994), and variability in solar forcing (Landscheidt 2001).

2.2 The Pacific Decadal Oscillation (PDO) and North Pacific Gyre Oscillation (NPGO)

The dominant mode of PDV is called the Pacific Decadal Oscillation (PDO) (Mantua et al. 1997). A warm PDO phase is characterized by cool SSTs in the central North Pacific and anomalously warm SSTs along the west coast of North America. Low SLP anomalies over the North Pacific cause enhanced counterclockwise winds, whereas high SLP over the northern subtropical Pacific cause enhanced clockwise winds. To characterize the temporal evolution of this mode, a PDO index has been defined as the leading principal component (PC) of monthly SST anomalies poleward of 20°N (Mantua et al. 1997). This index is marked by variability on interannual and decadal time scales, with some abrupt sign changes such as the 1976-77 climate shift. Even though the PDO index has been used widely to characterize North Pacific decadal variability, the processes underlying the temporal and spatial characteristics of the

PDO have not been clarified (Mantua and Hare 2002).

Recently, Di Lorenzo et al. (2008) defined a mode of climate variability in the Northeast Pacific termed the North Pacific Gyre Oscillation (NPGO). The NPGO climate pattern emerges as the second empirical orthogonal-principal component (EOF/PC) of both SSTA and SSHA over the region 180° - 110° W; 25° N- 62° N. The NPGO explains 22% and 8% of the SSTA and SSHA variance respectively (Di Lorenzo et al. 2008) and its index (second PC of SSHA) exhibits variability on decadal time scales. The spatial pattern of the NPGO shows a dipole structure (Figure 2a) associated with the intensification and weakening of the eastern and central branches of the subpolar and subtropical gyres in the North Pacific, as shown in Figure 2b. As mentioned before, the NPGO index explains observed variability in salinity and nutrients in the California Current System that are not fully explained by the PDO index (Di Lorenzo et al. 2008).

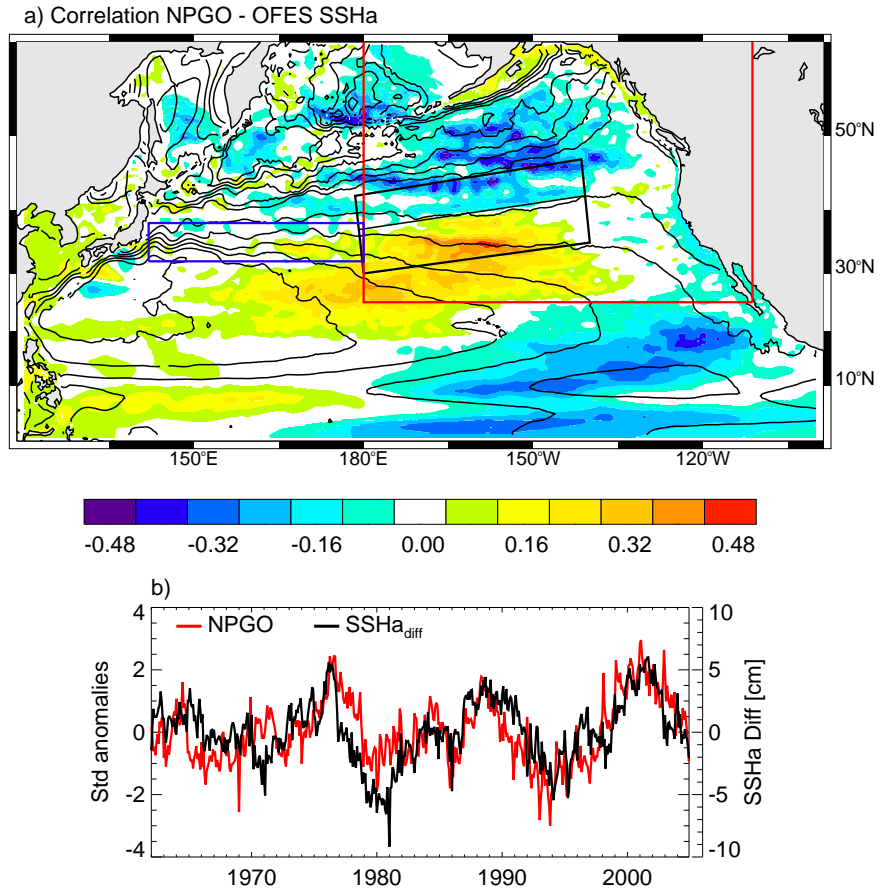


Figure 2: (a) Correlation map between the NPGO index and the OFES SSHa in the North Pacific (shaded contours). The red box delimits the region where the NPGO index was obtained. The contour lines represent the mean sea level. (b) Time series of the NPGO index (red line), and SSHa gradient in the black box on the left. This gradient represents the strength of the central/eastern branches of the subpolar and subtropical gyres.

CHAPTER III

DATA

Monthly sea surface height fields from a hindcast by the Ocean General Circulation Model (OGCM) for the Earth Simulator (OFES; Masumoto et al. 2004; Sasaki et al. 2008) are used in this study. The model extends from 75°S to 75°N with a horizontal resolution of 0.1° and 54 vertical levels, spanning the period 1950-2004. In this study, we analyze data from the 1962-2004 period. The OGCM was forced by surface wind stress, heat, and freshwater fluxes derived from daily National Centers for Environmental Prediction-National Center for Atmospheric Research (NCEP-NCAR) reanalysis (Kalnay et al. 1996), and a relaxation of surface salinity to the observed climatology. The model hindcast has been successfully used in previous studies to analyze different aspects of the decadal variability in the KOE (Nonaka et al. 2006; Taguchi et al. 2007). In particular, the observed southward shift and intensification of the Kuroshio and Oyashio jets after the 1976/77 climate shift of the North Pacific were detectable on the OFES output (Nonaka et al. 2006).

Surface wind stress from NCEP/NCAR reanalysis is used to represent the atmospheric forcing field. This dataset has a spatial resolution of 1.9° latitude x 1.875° longitude and covers the same time period as the OFES integration. Sea level pressure from NCEP/NCAR reanalysis with a 2.5° spatial resolution is also used to determine the principal modes of North Pacific atmospheric variability. TOPEX/Poseidon altimeter data (Ducet et al. 2000) from 1993-2004 is used for comparison with the OFES and the Rossby wave model output.

CHAPTER IV

KOE DECADAL VARIABILITY

The Kuroshio-Oyashio Extension has been identified in several studies as a region where strong ocean-atmosphere interaction takes place in the North Pacific (Latif and Barnett 1994; Pierce et al. 2001; Schneider et al. 2002; Qiu et al. 2007). It has been recognized as a region where the ocean circulation is most variable and where the subsurface ocean variability strongly affects sea surface temperature via vertical entrainment (Schneider et al. 2002) or horizontal advection by the Kuroshio and Oyashio jets (Qiu 2000; Seager et al. 2001; Kwon and Deser 2007). The Kuroshio Extension SSH is highly variable on interannual and decadal timescales. An EOF analysis of the zonal mean SSH anomalies averaged between 142°E-180° within 30°-45°N identified two dominant modes of SSH variability in the Kuroshio Extension (Taguchi et al. 2007). The first mode corresponds to changes in the mean latitudinal position of the Kuroshio Extension jet and shows the southward shift of the jet since the 1976/77 North Pacific climate shift. The second mode displays quasi-regular oscillations with a period of 10-15 yr (Figure 3, blue curve) and represents an intensification of the Kuroshio jet. It tracks very well the SSH meridional gradient in the latitudinal band of the KE jet core between 34.5° and 37°N (Figure 3, correlation coefficient = 0.71) (Taguchi et al. 2007).

We find that the quasi-regular decadal oscillations in the strength of the KOE are strongly coherent with the NPGO index. This is evident if we lag the time series of KOE mode-2 by approximately 3 years with the respect to the NPGO (Figure 4a). The correlation function between KOE mode-2 and NPGO at different lags (Figure 4b), shows that the maximum correlation (0.56) between the two time series occurs

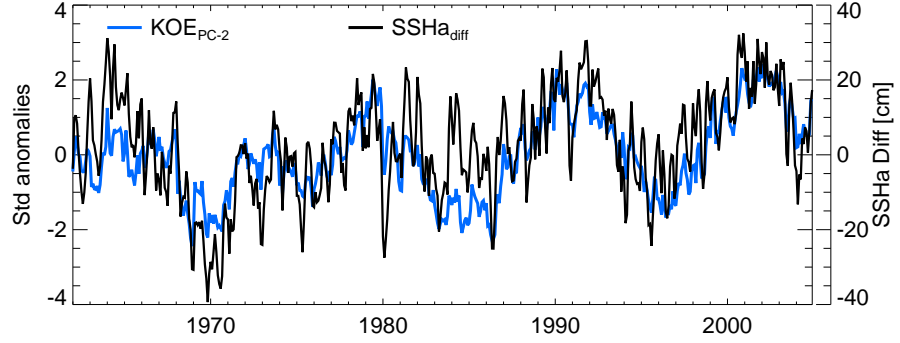


Figure 3: Time series of the second mode of variability in the KOE (blue curve), and SSHa gradient in the KOE region which corresponds to the strength of the Kuroshio Extension jet.

when NPGO leads KOE by 2.5 years. This lead-lag relationship is also evident in the space domain. By performing a time-lagged regression of the OFES North Pacific SSHa with the KOE mode-2 index we obtain spatial maps of the SSHa evolution associated with KOE mode-2 index. Figures 5a and 5b show correlation maps between SSHa and KOE mode-2 at 0 and -3 yr lag (NPGO leading). At lag 0 much of the north Pacific (north of 45°N) is occupied by negative correlations, whereas positive correlations span from the eastern to the western boundary in the KOE latitudinal band. However, 3 years before (Figure 5b), negative correlations extended from the eastern to the western boundary, (including the KOE latitudinal band), opposing positive correlations south of the Kuroshio region in a pattern that resembles the projection of the NPGO onto the SSHa (Figure 5c). The similitude between these correlation maps (pattern correlation coefficient = 0.75) indicates again that NPGO leads SSHa variability in the western boundary of the North Pacific, particularly the one associated with the KOE.

Twelve year lagged regression maps (not shown) suggest that KOE related SSH anomalies propagate from the eastern to the western boundary. A time-longitude plot of the lagged correlation maps at 35.25°N (Figure 5d) shows a propagation of anomalies from the eastern basin into the western North Pacific, confirming the east-west phase relationship and suggesting that ocean dynamics may be involved in carrying

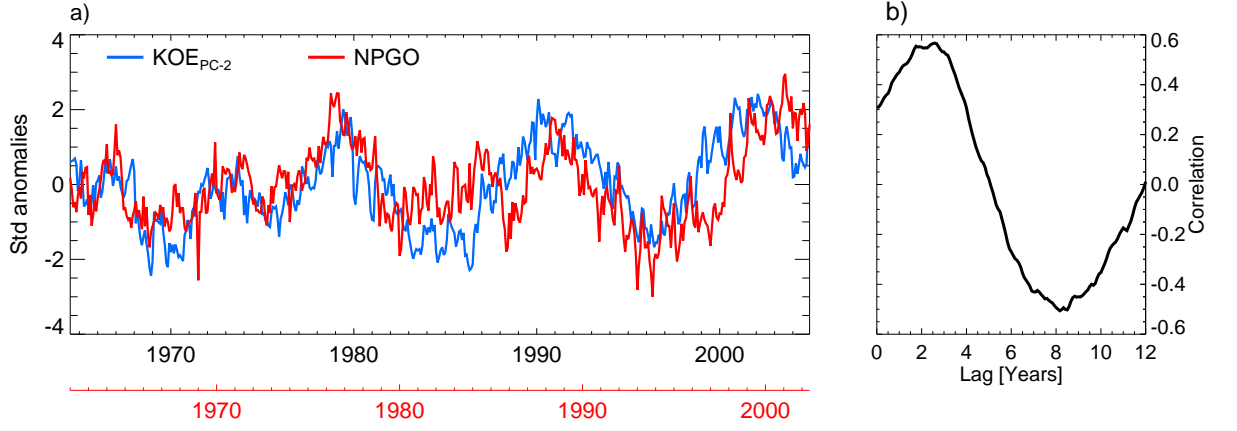


Figure 4: (a) NPGO (red) and KOE mode-2 (blue). The NPGO time axis is shifted 2.5 years forward in time to match the time of the maximum correlation coefficient between the two time series as shown on (b)

the NPGO signal from the east into the west. In the next section we will explore this relationship in a dynamical framework to determine whether the low frequency variability of SSHa in the western boundary and the NPGO share the same atmospheric forcing, namely the NPO.

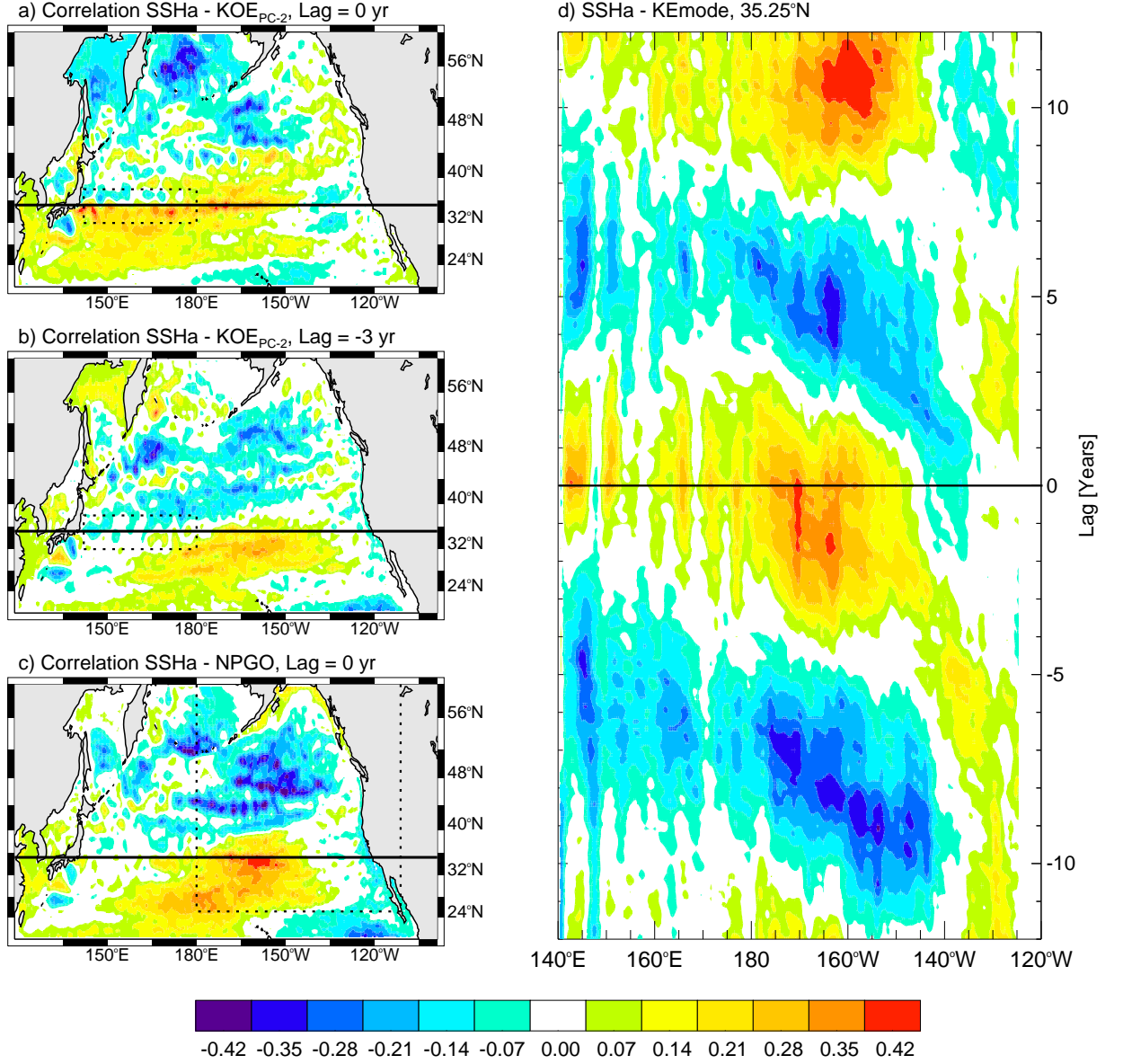


Figure 5: Spatial correlation pattern between (a) KOE mode-2 and OFES SSHa at 0 year lag and (b) at lag -3 yr (KOE leading). (c) Spatial correlation between NPGO and SSH anomalies at lag 0. (d) Time-longitude section at 35.25°N (black line on the left panel) of the lagged correlation maps between KOE mode-2 and SSHa.

CHAPTER V

DYNAMICS AND PROCESSES

On decadal timescales, the subsurface thermocline responds to changes at the surface Ekman pumping, i.e. changes of the wind stress curl. In the central North Pacific, anomalies of Ekman pumping associated with the Aleutian Low variability excite Rossby waves of the first baroclinic mode that propagate to the western boundary producing the observed decadal variability in the KOE (Deser et al. 1999; Miller et al. 1998; Seager et al. 2001). The concept of linear Rossby waves have been used widely to explain the oceanic response in the KOE to changes in the wind stress in the central Pacific. Using a simplified Rossby wave model, Schneider and Miller (2001) successfully hindcasted decadal anomalies of the thermocline depth and used it to predict KOE SST anomalies. Qiu (2003), used the same model to hindcast the SSHa field for the midlatitude North Pacific and found that the model was able to reproduce the low frequency SSHa variability in the KE region.

Assuming a 1-layer reduced-gravity model, under the long wave approximation, the linear vorticity equation is

$$\frac{\partial h}{\partial t} - c_R \frac{\partial h}{\partial x} = -\frac{g'}{g} w_e \quad (1)$$

where h is the SSH of interest, c_R is the zonal phase speed of the long baroclinic Rossby wave, g is gravity, g' is the reduced gravity, $w_e = \text{curl}(\tau/f\rho_0)$ is the Ekman pumping velocity, ρ is the density, f is the Coriolis parameter, and τ is the wind stress vector. A detailed derivation of this equation and its solution is presented by Qiu (2002). Integrating Eq. (1) along the baroclinic Rossby wave characteristic and

ignoring the SSHa signal from the eastern boundary, we obtain

$$h(x, t) = \frac{g'}{c_R \rho_0 g f} \int_x^0 w_e \left(x', t + \frac{x - x'}{c_R} \right) dx' \quad (2)$$

To hindcast $h(x, t)$ using Eq. (2), monthly wind stress anomalies from NCEP/NCAR reanalysis were used to compute w_e on the grid of the NCEP/NCAR reanalysis. Since the Rossby wave speed, c_R , varies with latitude, we use the values reported by Qiu (2003) for each latitude of the wind stress curl grid, i.e. from 0.041 ms^{-1} at 32°N to 0.024 ms^{-1} at 38°N . Finally, the reduced gravity value is $g' = 0.027 \text{ ms}^{-1}$.

Figure 6c shows the hindcasted monthly SSH anomalies averaged over the latitudinal band of the KOE, 32° - 38°N , as a function of time and longitude. For comparison, the SSH anomalies from OFES and satellite data from AVISO are shown in Figures 6a and 6b. In both plots, the western boundary is dominated by low-frequency SSH anomalies arriving from the east. This confirms the important role that remotely forced SSH anomalies play in modulating the KOE. As noted by Qiu and Chen (2005), the arrival of positive (negative) SSH anomalies to the KOE region corresponds to the strengthening (weakening) of the KE jet and the recirculation gyre. It is worth noting that the Rossby model only captures SSH anomalies due to changes in the wind stress and does not account for other dynamic processes such as instabilities and eddy-mean flow interaction present in the KOE region and evident in the OFES data. However, the Rossby model successfully hindcasts SSH anomalies in the KOE region as shown in Figure 4d, which compares time series of mean SSHa between 142°E - 180° from the Rossby model, OFES, and satellite. We note that the Rossby model has a particularly high skill from the 1970s onward.

Figure 6c also shows that most of the low-frequency SSH signals arriving at the western boundary originate near 150° - 160°W in the eastern/central North Pacific, which is the region where the wind stress curl has its largest amplitude in the North Pacific. Qiu (2003) showed that changes from positive to negative wind stress curl in the central Pacific correspond well to reversals of the PDO index, suggesting that

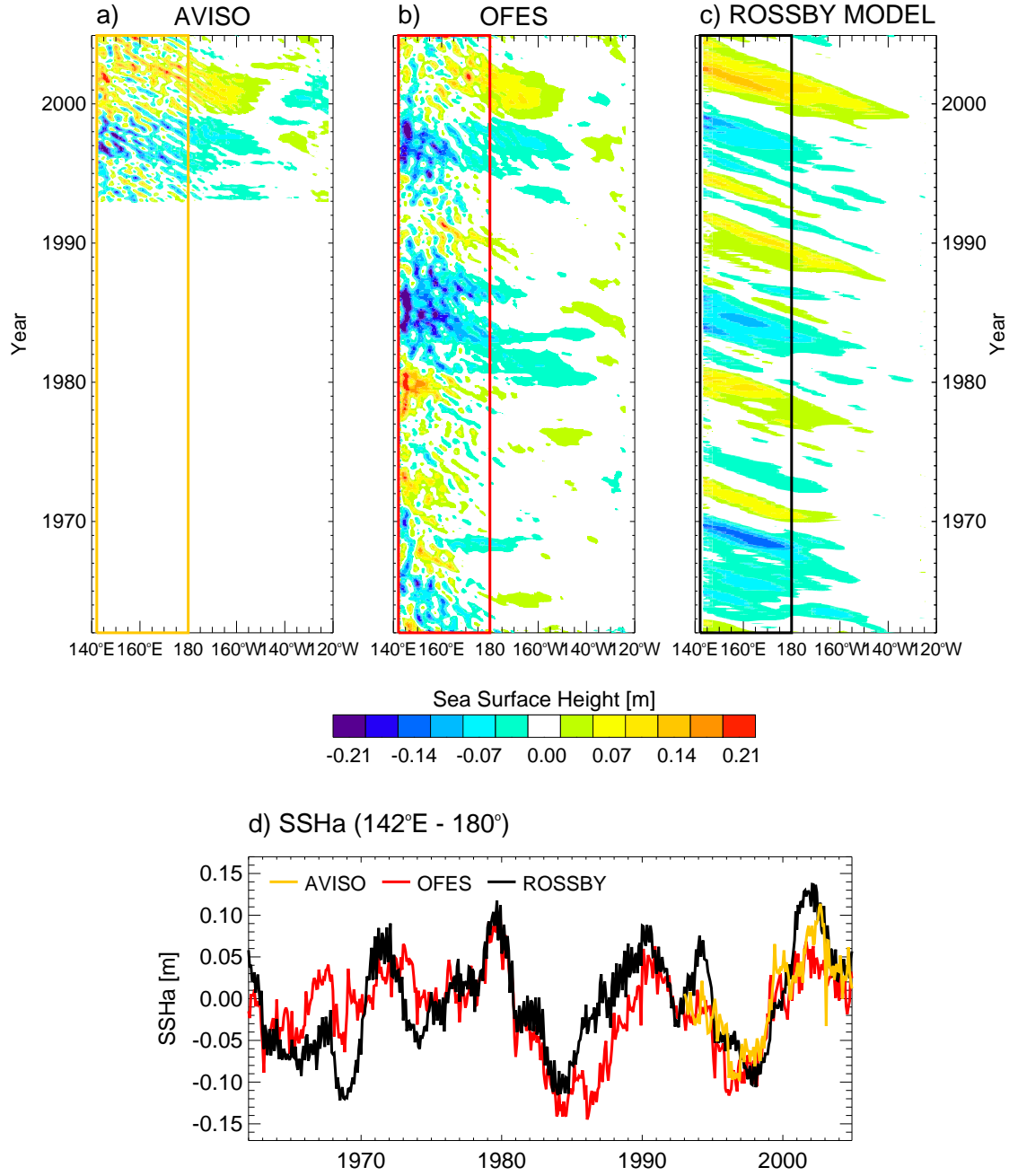


Figure 6: Time-longitude plots of SSHa averaged between 32.38-38.09N for (a) satellite data, (b) OFES hindcast, and (c) wind stress curl forced Rossby wave model. The yellow, red, and black boxes correspond to the KOE region where SSHa was averaged to obtain the time series in (d).

SSH variability in the KOE is related to the Pacific decadal oscillations.

To understand how Pacific decadal oscillations such as the PDO and the NPGO are linked to the SSH signals in the KOE, we decompose the wind stress curl into the two dominant modes of North Pacific atmospheric variability, the Aleutian Low mode and the NPO mode, which drive the PDO and NPGO respectively (Chhak et al. 2008). The decomposition was done using a regression analysis between the wind stress curl and each atmospheric mode. The regression coefficients were used to reconstruct, separately, the wind stress curl which is then used to force the Rossby model (Eq. 2). The time longitude plots of SSHa reconstructed using the two atmospheric modes (Figure 7) show westward propagation of SSH anomalies from the eastern/central Pacific. However, the sign of the arriving anomalies obtained with the Aleutian Low related wind stress curl (Figure 7a) and with the NPO forcing (Figure 7b) reveals important differences in the early 1980's and early 1990's.

A comparison of SSHa time series in the KOE region shows no correspondence between the SSHa obtained with the Aleutian Low forcing and the OFES hindcast (Figure 5c). In contrast, the SSHa obtained with the NPO forcing (Figure 8) closely tracks the OFES hindcast (correlation coefficient of 0.74), especially after 1985 when large amplitude fluctuations become more apparent. These results indicate that the NPO related wind stress curl anomalies explain an important fraction of the SSH decadal variability in the KOE. Because the NPO is the forcing pattern of the NPGO in the central and eastern North Pacific (Chhak et al. 2008; Di Lorenzo et al. 2008), this result gives further evidence that SSH variability in the KOE region is dynamically linked to NPGO.

Taguchi et al. (2007) isolate the KOE mode-2 and showed that it is associated with changes in the KE's strength but did not provide any forcing mechanism. By linking the NPGO forcing with SSH variability in the KOE we have revealed the forcing of the KOE mode-2 and provided physical foundations for this mode to exist.

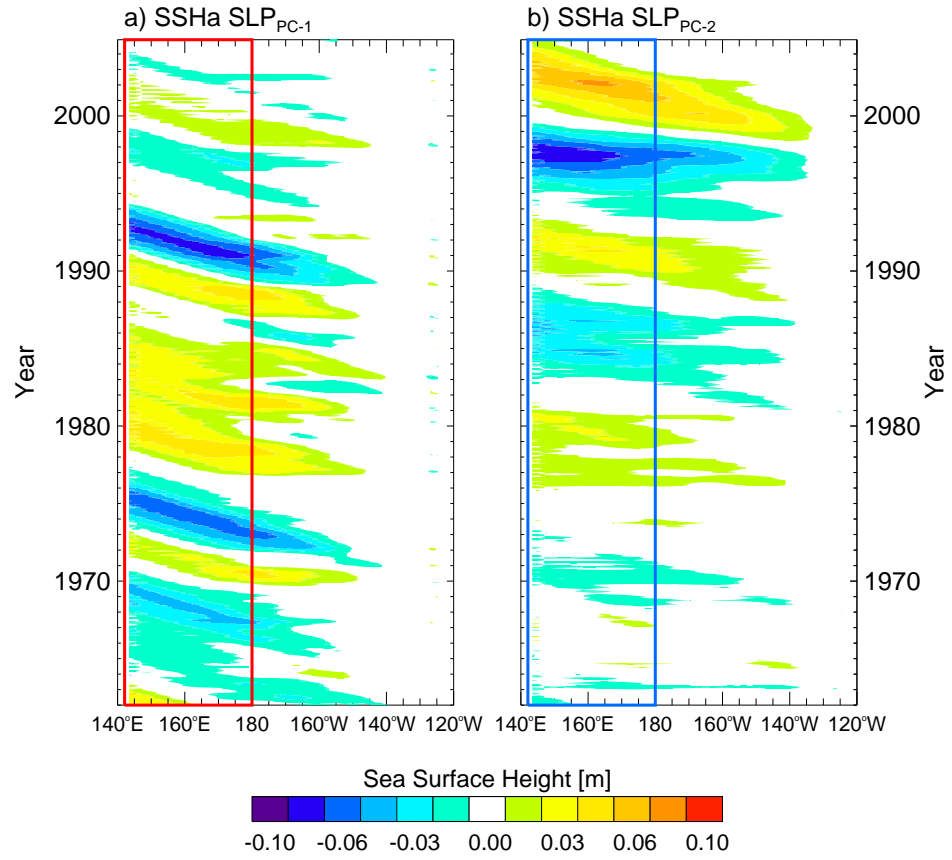


Figure 7: Time-longitude plots of SSHa averaged between 32.38-38.09N from (a) the Aleutian Low mode, and (b) the NPO related wind stress curl anomalies forced Rossby wave model.

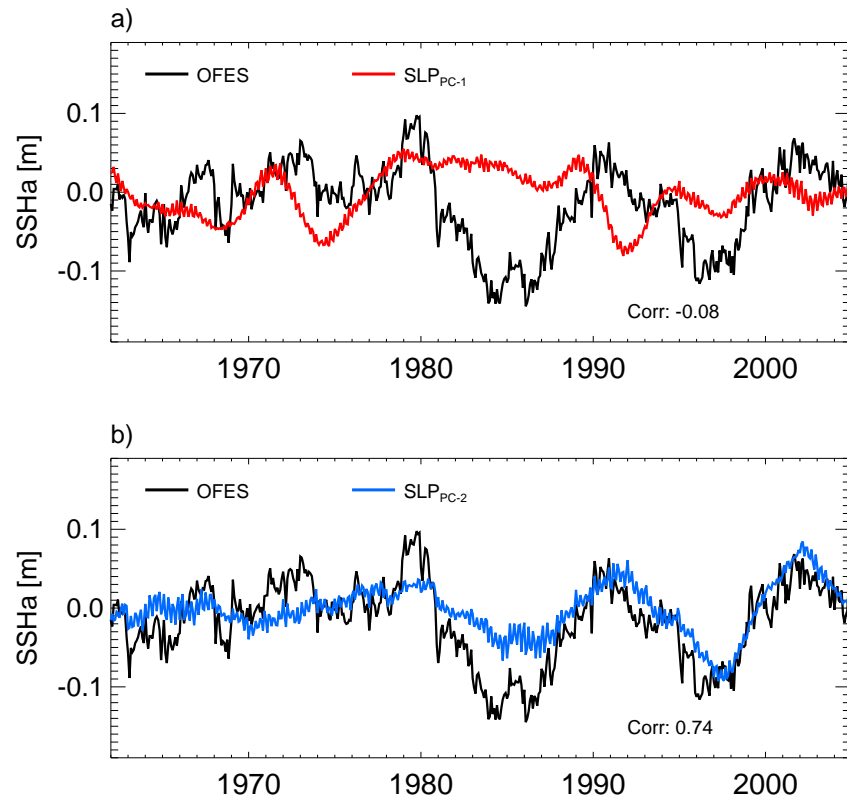


Figure 8: (a) Aleutian Low related KOE SSHa time series (red curve) and (b) NPO related KOE SSHa time series (blue curve). The black curve is the KOE SSHa time series from OFES.

Before concluding this section we must remark that the NPO wind stress curl forcing pattern isolated in Chhak et al. (2008) reveals some spatial differences with the NPO pattern inferred as the 2nd EOF of SLP in the North Pacific (Figs 9a,b). These differences reflect the different definitions used for the NPO. In Di Lorenzo et al. (2008) and Chhak et al. (2008), the NPO pattern emerges from a regression of the NPGO index with the atmospheric SLPa and is equivalent to the EOF-2 of wind stress curl over the Northeast Pacific quadrant (180° - 111° W; 25° N- 61° N). In this study we used the more recent definition of NPO by Linkin and Nigam (2008) as the 2nd EOF of North Pacific SLPa. Therefore, it is important to verify that both definitions of the NPO support the statement that NPGO is forced by NPO. Similar to Chhak et al. (2008), we use an AR-1 model forced by the NPO indices (Figs. 6c,d) to reconstruct the NPGO index. We find that both definitions of the NPO lead to a skillful reconstruction of the NPGO (Figs. 9e,f) with significant correlations of 0.46 (NPO defined as 2nd EOF of SLPa) and 0.71 (NPO defined as 2nd EOF of wind stress curl in the Northeast Pacific). Differences stem primarily from before the mid 1980s, when the forcing by the wind stress curl EOF reconstruct the NPGO accurately, while the skill of the sea level pressure EOF is not as accurate.

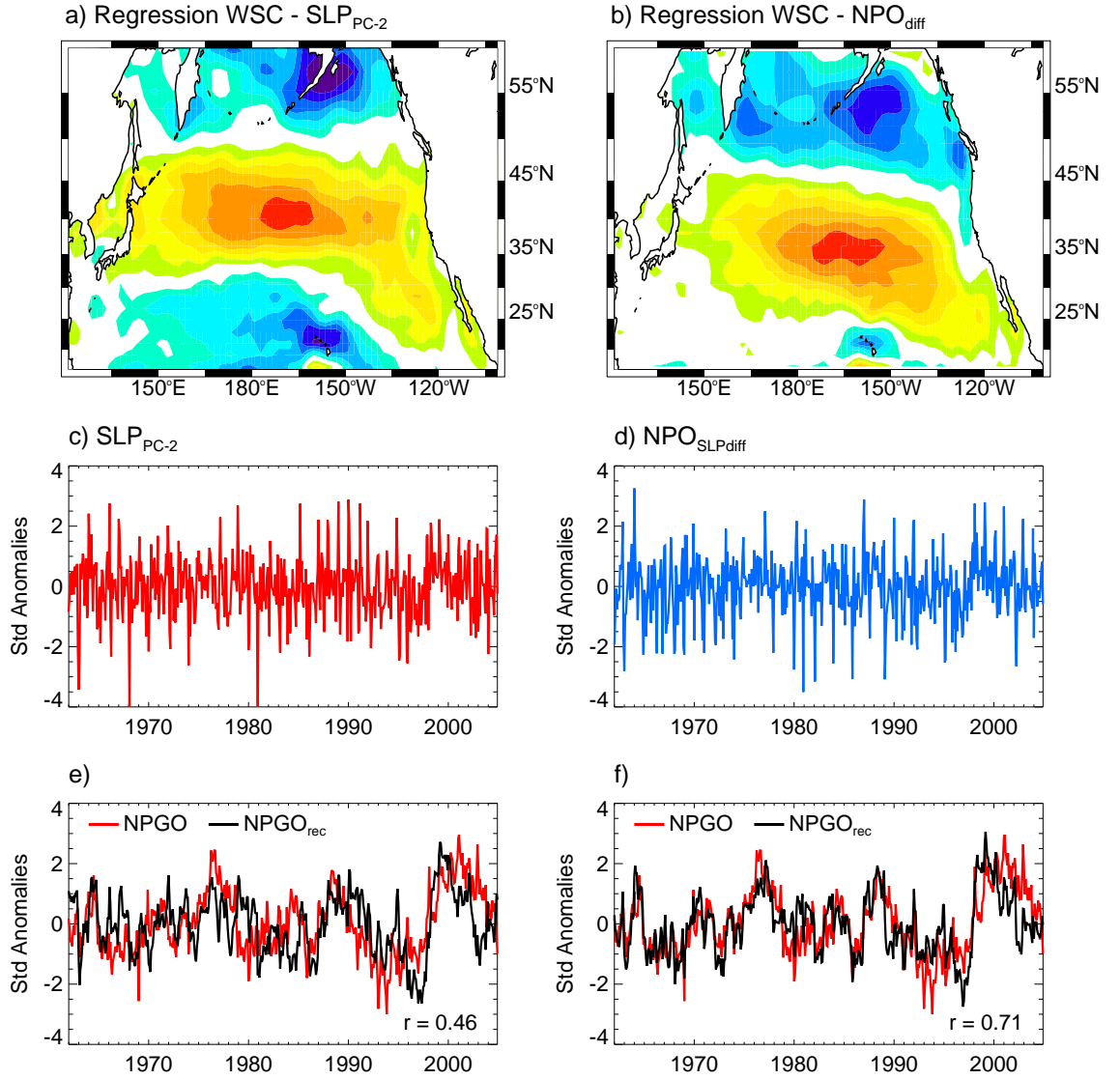


Figure 9: Wind stress curl correlation maps with the NPO as defined by Linkin and Nigam (2008) (a) and the NPO index defined by Chhak et al. (2008) (b). (c-d) Time series of the NPO index defined by these authors respectively and, (e-f) reconstructions of the NPGO index (black curve) using an AR-1 and the NPO indices as predictors.

CHAPTER VI

SUMMARY AND CONCLUSIONS

Using a hindcast experiment by the high resolution eddy-resolving OFES, along with sea level pressure and wind stress curl from the NCEP/NCAR reanalysis, we have studied the relationship between a recently identified mode of decadal variability in the Northeast Pacific, the North Pacific Gyre Oscillation (Di Lorenzo et al. 2008), and climate variability in the western boundary of the North Pacific. To achieve this goal, we analyzed the low-frequency variability of the SSH anomalies in the Kuroshio-Oyashio Extension region between 32° - 38° N and 142° E- 180° , which is characterized by two modes of variability. The first mode is associated with changes in the latitudinal position of the Kuroshio Extension jet, whereas the second one represents variations in the strength of the jet (Taguchi et al. 2007) and displays quasi-decadal oscillations comparable to those of the NPGO index.

To explore the east-west relationship, we used two different approaches. First, we looked for statistical evidence of the link between the NPGO and the modes of SSHa variability in the KOE, and secondly, using a simple linear Rossby wave model, we explored the dynamics underlying the east-west connection. The statistical approach, which involved time-lagged correlations, showed that the NPGO index leads the KOE SSHa variability associated with the strength of the KE jet by approximately 3 years. This result is supported by time-lagged spatial correlation maps that show how the NPGO pattern propagates from the eastern/central North Pacific towards the western boundary, highlighting the role of Rossby waves in carrying the signature of the NPGO across the eastern to the western boundary.

Linear baroclinic Rossby wave models have been used to link wind stress curl

anomalies in the eastern/central North with SSHa variability in the Kuroshio Extension (Qiu 2003; Schneider and Miller 2001). The success of these models has led to the hypothesis that Pacific decadal oscillations modulate decadal variability on the western boundary via changes in the wind stress curl field of the eastern/central North Pacific. Here we used a linearized Rossby wave model to hindcast the SSHa in the KOE region and determine to what extent wind stress curl anomalies associated with the forcing of the NPGO, namely the NPO, drive the low-frequency SSHa variability in that region. By decomposing the wind stress curl field into the first two dominant SLP modes of North Pacific variability - the Aleutian Low and the NPO mode -, we found that a significant fraction of the KOE SSHa is explained by NPO related wind stress curl anomalies, whereas the Aleutian Low SSH related anomalies did not compare well with the OFES KOE SSHa. These results lead us to conclude that the eastern Pacific NPGO and a fraction of the western Pacific KOE SSHa variability share the same atmospheric forcing, i.e. the NPO, and that SSH variability in the KE's strength is modulated by this atmospheric mode and not by the Aleutian Low.

Our findings have implications for the predictability of the western North Pacific Ocean climate. Schneider and Miller (2001) showed that wintertime sea surface temperature anomalies in the Kuroshio-Oyashio could be predicted at lead times of up to 2 years, using the wind stress over the North Pacific and oceanic Rossby wave dynamics. Therefore, the NPGO-KOE connection can be used to predict western boundary climate fluctuations on decadal time scales. Additionally, the results of this study could be extended to determine to what extent, and by what mechanisms, modes of North Pacific variability such as the NPGO, drive coherent changes in the marine ecosystems of the KOE region.

REFERENCES

- [1] Alexander, M. A., I. Blade, M. Newman, J. R. Lanzante, N. C. Lau, and J. D. Scott “The atmospheric bridge: The influence of ENSO teleconnections on air-sea interaction over the global oceans”. *J. Climate*, 15, 2205-2231, 2002
- [2] Alexander, M. A., “Midlatitude atmosphere-ocean interaction during El Niño. Part I: The North Pacific Ocean”. *J. Climate*, 5, 944-958, 1992
- [3] Barlow, M., S. Nigam, and E. H. Berbery, “ENSO, Pacific decadal variability, and US summertime precipitation, drought, and stream flow”. *J. Climate*, 14, 2105-2128, 2001
- [4] Chhak, K., E. Di Lorenzo, P. Cummins, and N. Schneider, “Forcing of low-frequency ocean variability in the Northeast Pacific,” *J. Climate in press*.
- [5] Chiang, J. C. H. and D. J. Vimont, “Analogous Pacific and Atlantic meridional modes of tropical atmosphere-ocean variability,” *J. Climate*, 17, 4143-4158, 2004.
- [6] Davis, R. E., “Predictability of sea-surface temperature and sea-level pressure anomalies over North Pacific Ocean,” *J. Phys. Oceanogr.*, 6, 249-266, 1976.
- [7] Deser, C., and M. L. Blackmon, “On the relationship between Tropical and North Pacific sea-surface temperature variations,” *J. Climate*, 8, 1677-1680, 1995.
- [8] Deser, C., M. A. Alexander, and M. S. Timlin, “Evidence for a wind-driven intensification of the Kuroshio Current extension from the 1970s to the 1980s,” *J. Climate*, 12, 1697-1706, 1999.
- [9] Di Lorenzo, E., and Coauthors, “North Pacific Gyre Oscillation links ocean climate and ecosystem change,” *Geophys. Res. Lett.*, 35, 6, 2008.

- [10] Ducet, N., P. Y. Le Traon, and G. Reverdin, "Global high-resolution mapping of ocean circulation from TOPEX/Poseidon and ERS-1 and-2," *J. Geophys. Res.*, 105, 19477-19498, 2000.
- [11] Fiedler, P. C., "Environmental change in the eastern tropical Pacific Ocean: review of ENSO and decadal variability," *Mar. Ecol. Prog. Ser.*, 244, 265-283, 2002.
- [12] Francis, R. C., S. R. Hare, A. B. Hollowed, and W. S. Wooster, "Effects of interdecadal climate variability on the oceanic ecosystems of the NE Pacific," *Fish. Oceanogr.*, 7, 1-21, 1998.
- [13] Frankignoul, C. and K. Hasselmann, "Stochastic climate models. Part II: application to sea-surface temperature anomalies and thermocline variability," *Tellus*, 29, 289-305, 1977.
- [14] Graham, N. E., "Decadal-scale climate variability in the Tropical and North Pacific during the 1970s and 1980s: observations and model results," *Climate Dyn.*, 10, 135-162, 1994.
- [15] Gu, D. F. and G. H. Philander, "Interdecadal climate fluctuations that depend on exchanges between the tropics and extratropics," *Science*, 805-807, 1994.
- [16] Hasselmann, K., "Stochastic climate models. Part I. Theory," *Tellus.*, 28, 473-485, 1976.
- [17] Kalnay, E., and Coauthors, "The NCEP/NCAR 40-year reanalysis project," *Bull. Amer. Meteor. Soc.*, 77, 437-471, 1996.
- [18] Kwon, Y. O. and C. Deser, "North Pacific decadal variability in the Community Climate System Model version 2," *J. Climate*, 20, 2416-2433, 2007.

- [19] Landscheidt, T., "Trends in Pacific Decadal Oscillation subjected to solar forcing," <http://www.john-daly.com/theodor/pdotrend.htm>, 2001.
- [20] Latif, M. and T. P. Barnett, "Causes of decadal climate variability over the North Pacific and North America," *Science*, 266, 634-637, 1994.
- [21] Latif, M. and T. P. Barnett, "Decadal climate variability over the North Pacific and North America: Dynamics and predictability," *J. Climate*, 9, 2407-2423, 1996.
- [22] Linkin, M. E. and S. Nigam, "The north pacific oscillation-west Pacific teleconnection pattern: mature-phase structure and winter impacts," *J. Climate*, 21, 1979-1997, 2008.
- [23] Mantua, N. J., S. R. Hare, Y. Zhang, J. M. Wallace, and R. C. Francis, "A Pacific interdecadal climate oscillation with impacts on salmon production," *Bull. Amer. Meteor. Soc.*, 78, 1069-1079, 1997.
- [24] Mantua, N. J., and S. R. Hare, "The Pacific decadal oscillation," *J. Oceanogr.*, 58, 35-44, 2002.
- [25] Masumoto, Y., and Coauthors, "A fifty-year eddy-resolving simulation of the World Ocean - preliminary outcomes of the OFES (OGCM for the Earth Simulator), " *J. Earth Simulator*, 1, 35-56, 2004.
- [26] Meyers, S. D., M. A. Johnson, M. Liu, J. J. Obrien, and J. L. Spiesberger, "Interdecadal variability in a numerical model of the northeast Pacific Ocean 1970-89, " *J. Phys. Oceanogr.*, 26, 2635-2652, 1996.
- [27] Miller, A. J., D. R. Cayan, T. P. Barnett, and N. E. Graham, and J. M. Oberhuber, "Interdecadal variability of the Pacific Ocean: model response to observed heat flux and wind stress anomalies, " *Climate Dyn.*, 9, 287-302, 1994.

- [28] ———, D. R. Cayan, and W. B. White, “A westward-intensified decadal change in the North Pacific thermocline and gyre-scale circulation,” *J. Climate*, 11, 3112-3127, 1998.
- [29] ———, and N. Schneider, “Interdecadal climate regime dynamics in the North Pacific Ocean: theories, observations and ecosystem impacts” *Prog. Oceanogr.*, 47, 355-379, 2000.
- [30] ———, F. Chai, S. Chiba, J. R. Moisan, and D. J. Neilson, “Decadal-scale climate and ecosystem interactions in the North Pacific Ocean”. *J. Oceanogr.*, 60, 163-188, 2004.
- [31] Nonaka, M., H. Nakamura, Y. Tanimoto, T. Kagimoto, and H. Sasaki, “Decadal variability in the Kuroshio-Oyashio Extension simulated in an eddy-resolving OGCM,” *J. Climate*, 19, 1970-1989, 2006.
- [32] Nakamura H., G. Lin, and T. Yamagata, “Decadal climate variability in the North Pacific during the recent decades,” *Bull. Amer. Meteor. Soc.*, 78, 2215-2225, 1997.
- [33] Pierce, D. W., T. P. Barnett, N. Schneider, R. Saravanan, D. Dommenges, and M. Latif, “The role of ocean dynamics in producing decadal climate variability in the North Pacific,” *Climate Dyn.*, 18, 51-70, 2001.
- [34] Qiu, B., “Interannual variability of the Kuroshio Extension system and its impact on the wintertime SST field,” *J. Phys. Oceanogr.*, 30, 1486-1502, 2000.
- [35] ———, “Large-scale variability in the midlatitude subtropical and subpolar North Pacific Ocean: observations and causes,” *J. Phys. Oceanogr.*, 32, 353-375, 2002.

- [36] ———, “Kuroshio Extension variability and forcing of the Pacific decadal oscillations: responses and potential feedback,” *J. Phys. Oceanogr.*, 33, 2465-2482, 2003.
- [37] ——— and S. M. Chen, “Variability of the Kuroshio Extension jet, recirculation gyre, and mesoscale eddies on decadal time scales,” *J. Phys. Oceanogr.*, 35, 2090-2103, 2005.
- [38] ———, N. Schneider, and S. M. Chen, “Coupled decadal variability in the North Pacific: an observationally constrained idealized model,” *J. Climate*, 20, 3602-3620, 2007.
- [39] Rogers, J. C., “The North Pacific Oscillation”. *J. Climatol.*, 1, 39-58, 1981.
- [40] Sasaki, H., M. Nonaka, Y. Masumoto, Y. Sasai, H. Uehara, and H. Sakuma, “An eddy-resolving hindcast simulation of the quasiglobal ocean from 1950 to 2003 on the Earth Simulator, ” High Resolution Numerical Modelling of the Atmosphere and Ocean, K. Hamilton and W. Ohfuchi, Eds., Springer-Verlag, 157–185, 2008.
- [41] Schneider, N. and A. J. Miller, “Predicting western North Pacific Ocean climate,” *J. Climate*, 14, 3997-4002, 2001.
- [42] ———, and B. D. Cornuelle, “The forcing of the Pacific decadal oscillation,” *J. Climate*, 18, 4355-4373, 2005.
- [43] ———, A. J. Miller, and D. W. Pierce, “Anatomy of North Pacific decadal variability,” *J. Climate*, 15, 586-605, 2002.
- [44] Seager, R., Y. Kushnir, N. H. Naik, M. A. Cane, and J. Miller, “Wind-driven shifts in the latitude of the Kuroshio-Oyashio Extension and generation of SST anomalies on decadal timescales,” *J. Climate*, 14, 4249-4265, 2001.

- [45] Taguchi, B., S. P. Xie, N. Schneider, M. Nonaka, H. Sasaki, and Y. Sasai, “Decadal variability of the Kuroshio Extension: Observations and an eddy-resolving model hindcast,” *J. Climate*, 20, 2357-2377, 2007.
- [46] Trenberth, K. E., “Recent observed interdecadal climate changes in the northern-hemisphere,” *Bull. Amer. Meteor. Soc.*, 71, 988-993, 1990.
- [47] Trenberth, K. E. and J. W. Hurrell, “Decadal atmosphere - ocean variations in the Pacific,” *Climate Dyn.*, 9, 303-319, 1994.
- [48] Vimont, D. J., D. S. Battisti, and A. C. Hirst, “Footprinting: A seasonal connection between the tropics and mid-latitudes,” *Geophys. Res. Lett.*, 28, 3923-3926, 2001.
- [49] ———, J. M. Wallace, and D. S. Battisti, “The seasonal footprinting mechanism in the Pacific: Implications for ENSO,” *J. Climate*, 16, 2668-2675, 2003.
- [50] Walker, G. and E. Bliss, “World weather V,” *Mem. Roy. Meteor. Soc.*, 4, 53-85, 1932.
- [51] Weare, B. C., A. R. Navato, and R. E. Newell, “Empirical orthogonal analysis of Pacific sea-surface temperatures,” *J. Phys. Oceanogr.*, 6, 671-678, 1976.